

2

3 **Hydrophobicity of Hemp Shiv treated with Sol-gel Coatings**

4

5 **Atif Hussain^{a, b,*}, Juliana Calabria-Holley^a, Diane Schorr^b, Yunhong Jiang^a, Mike Lawrence^a,**
6 **Pierre Blanchet^b**

7 ^aBRE Centre for Innovative Construction Materials, Department of Architecture and Civil
8 Engineering, University of Bath, Bath BA2 7AY, UK

9 ^bNSERC Industrial Research Chair on Ecoresponsible Wood Construction, Department of Wood
10 and Forest Sciences, Université Laval, Quebec, QC, G1V 0A6, Canada

11 *Corresponding Author: Atif Hussain (A.Hussain@bath.ac.uk)

12

13 **Abstract**

14 This is the first time sol-gel technology is used in the treatment of hemp shiv to develop
15 sustainable thermal insulation building materials. The impact on the hydrophobicity of hemp shiv
16 by depositing functionalised sol-gel coatings using hexadecyltrimethoxysilane (HDTMS) has been
17 investigated. Bio-based materials have tendency to absorb large amounts of water due to their
18 hydrophilic nature and highly porous structure. In this work, the influence of catalysts, solvent
19 dilution and HDTMS loading in the silica sols on the hydrophobicity of hemp shiv surface has been
20 reported. The hydrophobicity of sol-gel coated hemp shiv increased significantly when using acid
21 catalysed sols which provided water contact angles of up to 118° at 1% HDTMS loading. Ethanol
22 diluted sol-gel coatings enhanced the surface roughness of the hemp shiv by 36% as observed
23 under 3D optical profilometer. The XPS results revealed that the surface chemical composition of
24 the hemp shiv was altered by the sol-gel coating, blocking the hydroxyl sites responsible for
25 hydrophilicity.

26

27 **Keywords**

28 Sol-gel, hydrophobicity, coatings, surface roughness, hemp shiv

29

30

31 **1. Introduction**

32 Wettability of a solid surface is governed by a combination of chemical composition and geometric
33 structure of the surface [1,2]. The interplay between surface chemistry and surface roughness
34 has been an active research topic for enhancing the hydrophobicity of cellulose based materials.

35

36 The woody core of the hemp plant (*Cannabis Sativa* L.) known as shiv has gained interest in the
37 building industry during the recent years for production of lightweight composites. Hemp shiv
38 based composites have interesting properties such as thermal [3], hygroscopic [4], mechanical,
39 acoustic [5] and biodegradability [6].

40

41 Hemp shiv are generally very porous with low density tending to absorb large amounts of water.
42 Previous studies have reported that hemp shiv not only has higher water absorption rate but also
43 absorb high amounts of water in the very first minutes compared to different plant materials [7].
44 Moreover, the presence of cellulose, hemicellulose and lignin in bio-based materials contributes
45 to the presence of hydroxyl groups in their structure. This leads to certain disadvantages of using
46 bio-based materials making them incompatible with hydrophobic thermoset/thermoplastic
47 polymers [8]. High moisture uptake also encourages colonial fungal growth resulting in cell wall
48 degradation and lower durability of the material [9].

49

50 The major constituents of industrial hemp shiv are: cellulose (44%), hemicellulose (18-27%), lignin
51 (22-28%) and other components such as extractives (1-6%) and ash (1-2%) [10,11]. Cellulose is
52 a semi crystalline polysaccharide consisting of linear chain of several D-glucose units linked
53 together by β (1–4) glucosidal bond. Cellulose contains free hydroxyl groups, and since they form
54 the major structural component of hemp shiv, they are responsible for the extreme hydrophilic
55 behaviour.

56

57 One of the mechanism to convert cellulose-based material from hydrophilic to hydrophobic
58 involves chemical modification to block the hydroxyl groups of the cell wall thereby reducing water
59 sorption sites. Treatments include acetylation [12], silanization [13] and in situ polymerization [14]
60 that involve incorporation of materials into the cell wall blocking the voids accessible to water
61 molecules. Other treatments methods that are known to enhance the water repellence are plasma
62 etching, lithography, electrospinning and sol-gel treatment that endow the material with nano-
63 scale surface roughness [15].

64
65 Chemical pre-treatment of natural plant materials have reported better bonding with polymer
66 matrix interface due to improvement of their hydrophobic characteristics [16]. There is a need to
67 develop a novel treatment method for hemp shiv to enhance its water resistance thereby
68 improving the shiv-binder interfacial adhesion and reduce its susceptibility to decay. The sol-gel
69 technique is a highly versatile method to deposit silica based coatings possessing single or multi
70 functionality [17]. These thin mesoporous coatings have high structural homogeneity and their
71 adhesion can be tailored to different substrates.

72
73 Sol-gel based hydrophobic and water repellent coatings have been investigated on different bio-
74 based materials such as wood [18] and cellulosic fibres [19], however for hemp shiv this is the
75 first time. The reactive hydroxyl groups present in the polysiloxane network of the sol-gel combine
76 with the hydroxyl groups of cellulose through a covalent bond. This study successfully delivers a
77 sol-gel modified hemp shiv material of hydrophobic character through a simple and inexpensive,
78 one step dip-coating method.

79

80 **2. Experimental**

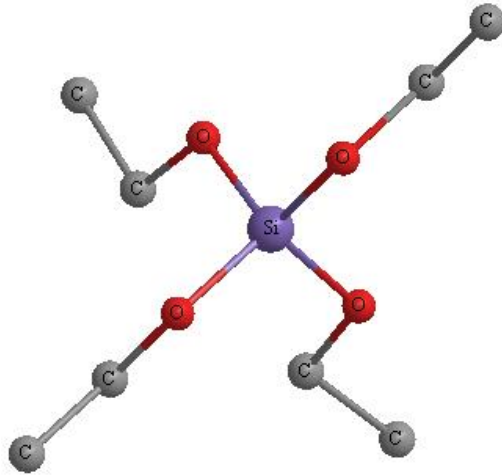
81

82 **2.1 Materials**

83 Hemp shiv used in this study was received from MEM Inc., manufacturer of ecological materials
84 based in Rimouski, Canada. Tetraethyl orthosilicate (TEOS, 98%) and hexadecyltrimethoxysilane
85 (HDTMS, 85%) were obtained from Sigma-Aldrich. Anhydrous ethanol was purchased from
86 Commercial Alcohols, Canada. Hydrochloric acid (HCl, 38%) and nitric acid (HNO₃, 70%) were
87 obtained from Anachemia, VWR, Canada. All chemicals were used as received without further
88 purification.

89

(A)



90

(B)

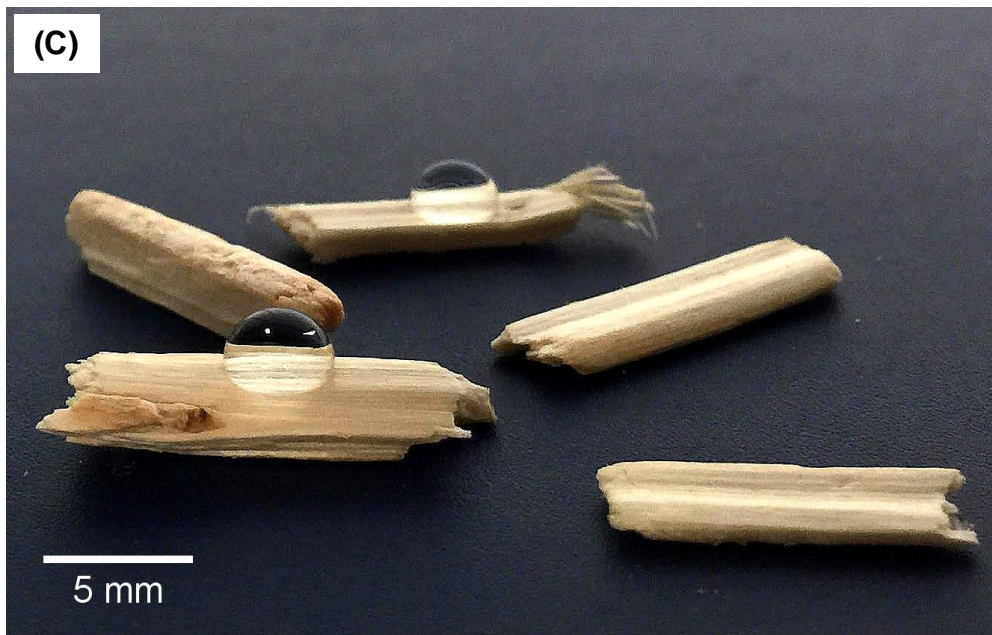


91

92

93

(C)



94

95

Figure 1. 3D structure of a (A) TEOS molecule, (B) HDTMS molecule; and (C) water on coated hemp shiv samples.

96

97 It is known that HDTMS may not be able to penetrate the outer surface layers of the cell wall due
98 to its high molecular weight [18]. Due to this, the hydrophobicity would be compromised and it can
99 be predicted that the coating might not be robust. Moreover, using only HDTMS would be highly
100 expensive and would not be of interest to the construction industry. For these reasons, it was
101 considered inappropriate to make a comparative study using purely HDTMS.

102

103

104 **2.2 Preparation of the hydrophobic coatings**

105 The silica based sol-gel was synthesised by hydrolysis and condensation of TEOS in ethanol and
106 water. The reaction was catalysed using 0.005M acid (HCl/ HNO₃). Two sets of silica sols were
107 prepared based on the difference in concentration of ethanol. The first set of formulations (sols
108 A) were prepared stirring 1M TEOS in a mixture of 4M water and 4M ethanol. For the preparation
109 of the second set of formulations (sols B), 1M TEOS was added to 4M water and 16M ethanol.
110 After the preparation of both sets of silica formulations, the hydrophobic agent HDTMS was added
111 in concentrations of 0.5-4 wt% of the sol. These mixtures of silica sol and HDTMS were stirred at
112 300 rpm for at least 20 minutes before performing the dip-coating process. All the sols were
113 prepared at 40 °C and atmospheric pressure. The sols were allowed to cool down to room
114 temperature and the pH was recorded.

115

116 The sols aged for 48 hours in closed container at room temperature before the dip-coating
117 process. Gelation took place in-situ in which pieces of hemp shiv were dipped in the sol for 10
118 min and then carefully removed and transferred onto a Petri dish. The samples were placed at
119 room temperature for one hour and then dried at 80 °C for one hour. A schematic illustration of
120 the HDTMS modified silica sol-gel coating is shown in Figure 1.

121

122 As for the preparation of the pure sol-gel specimen, the sol aged in a container at room
123 temperature until gel point. The gel-point was taken as the time when the sol did not show any
124 movement on turning the container upside down. The gel-time and pH for all the prepared sols
125 are reported in Table 1.

126

127 *Table 1. Composition of the prepared sol-gel formulations and their properties.*

FORMULATION	CATALYST	ETHANOL CONC. (M)	HDTMS CONC. (wt%)	GEL TIME (DAYS)	pH
sol A-1	HCl	4.0	4.0	178	1.87
sol A-2	HCl	4.0	2.0	116	1.82
sol A-3	HCl	4.0	1.0	101	1.78
sol A-4	HCl	4.0	0.5	101	1.85
sol A-5	HNO ₃	4.0	4.0	150	1.73
sol A-6	HNO ₃	4.0	2.0	112	1.87
sol A-7	HNO ₃	4.0	1.0	101	1.92
sol A-8	HNO ₃	4.0	0.5	101	1.92
sol B-1	HCl	16.0	4.0	>180	1.64
sol B-2	HCl	16.0	2.0	>180	1.68
sol B-3	HCl	16.0	1.0	>180	1.67
sol B-4	HCl	16.0	0.5	>180	1.72
sol B-5	HNO ₃	16.0	4.0	>180	1.70
sol B-6	HNO ₃	16.0	2.0	>180	1.76
sol B-7	HNO ₃	16.0	1.0	>180	1.81
sol B-8	HNO ₃	16.0	0.5	>180	1.83

128

129 **2.3 Contact Angle Measurements**

130 The water contact angle (WCA) of uncoated and coated hemp shiv samples were measured using
 131 a contact angle meter (First Ten Ångstroms USA, FTA200 series). The sessile drop method was
 132 employed and the contact angle was determined on at least three different positions for each
 133 sample (coated substrate). The volume of the water droplets was 5µl for the contact angle
 134 measurements. The average value was adopted as a final value. Images were captured and
 135 analysed using the FTA32 Video 2.0 software. All the measurements were performed at room
 136 temperature (24 ± 1 °C).

137

138 **2.4 Surface Roughness**

139 The topography and surface roughness of the samples was obtained using a 3D optical
140 profilometer (Bruker Nano GmbH Germany, ContourGT-K series). The surface roughness was
141 measured over an area at 0.25*0.30 mm² in non-contact mode at 20X magnification. Vision 64
142 on board software was then employed to analyse these data and calculate the roughness
143 parameters. The readings were taken on at least three different positions for each sample and
144 the average value was reported as the final value.

145

146 **2.5 X-ray photoelectron spectroscopy (XPS)**

147 The surface elemental and chemical composition of the samples were analysed using XPS. Prior
148 to XPS analysis, samples were oven-dried at 80 °C for 96 hours. XPS spectra of uncoated and
149 sol-gel coated hemp shiv were recorded with an X-ray photoelectron spectrometer (Kratos Axis
150 Ultra, UK). All spectra were collected using a monochromatic Al K α X-ray source operated at 300
151 watts. The lateral dimensions of the samples were 800 microns x 400 microns, corresponding to
152 those of the Al K α X-ray used, and probing depth was approximately 5 nanometres. For each
153 sample, two spectra were recorded: (i) survey spectra (0–1150 eV, pass energy 160 eV, and step
154 size 1eV) recorded for apparent composition calculation; and (ii) high-resolution C1s, O1s and Si
155 2p spectra (within 20 eV, pass energy 20 eV and step size within 0.05eV) recorded to obtain
156 information on chemical bonds. Calculation of the apparent relative atomic concentrations is
157 performed with the CasaXPS software. Peak fitting is performed with CasaXPS, which
158 automatically and iteratively minimizes the difference between the experimental spectrum and the
159 calculated envelope by varying the parameters supplied in a first guess.

160

161 **2.6 Scanning Electron Microscopy**

162 The surface morphology of the specimens was characterised using a scanning electron
163 microscopy (SEM), JEOL corporation - Japan Model JSM-6360 operating at 25 kV. The
164 specimens were coated with gold to achieve maximum magnification of textural and
165 morphological characteristics.

166

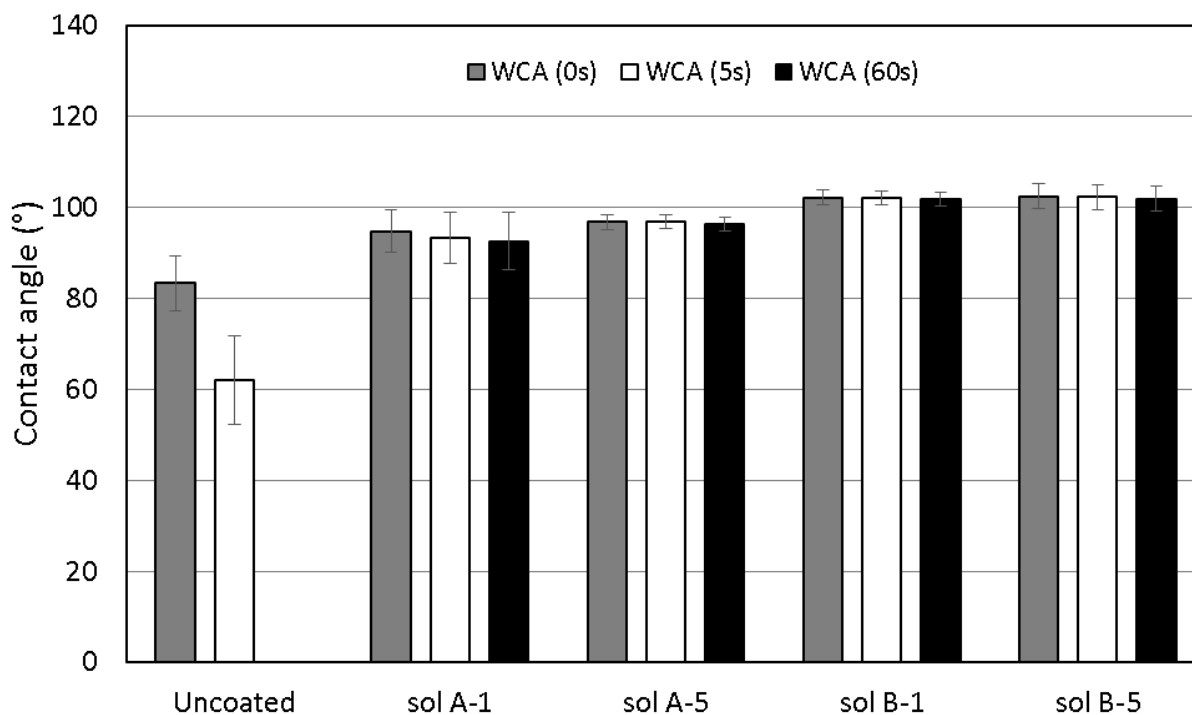
167

3. Results

3.1 Hydrophobicity of sol-gel coatings

169 The water contact angle was determined as soon as the water droplet encountered the sol-gel
170 coated hemp shiv surface. The sol-gel coatings with high HDTMS loadings (4 wt%) and varying
171 concentration of ethanol are compared in Figure 2. It can be seen that uncoated shiv has an
172 extremely hydrophilic surface and water droplet sinks into the substrate reducing the WCA in a
173 short time. The sol-gel coatings yield hydrophobicity to the hemp shiv by maintaining a stable
174 contact angle over 60 seconds.

175



176

177 *Figure 2. Hydrophobicity of hemp shiv surface treated with different sol-gel coatings over 60 seconds of water contact.*

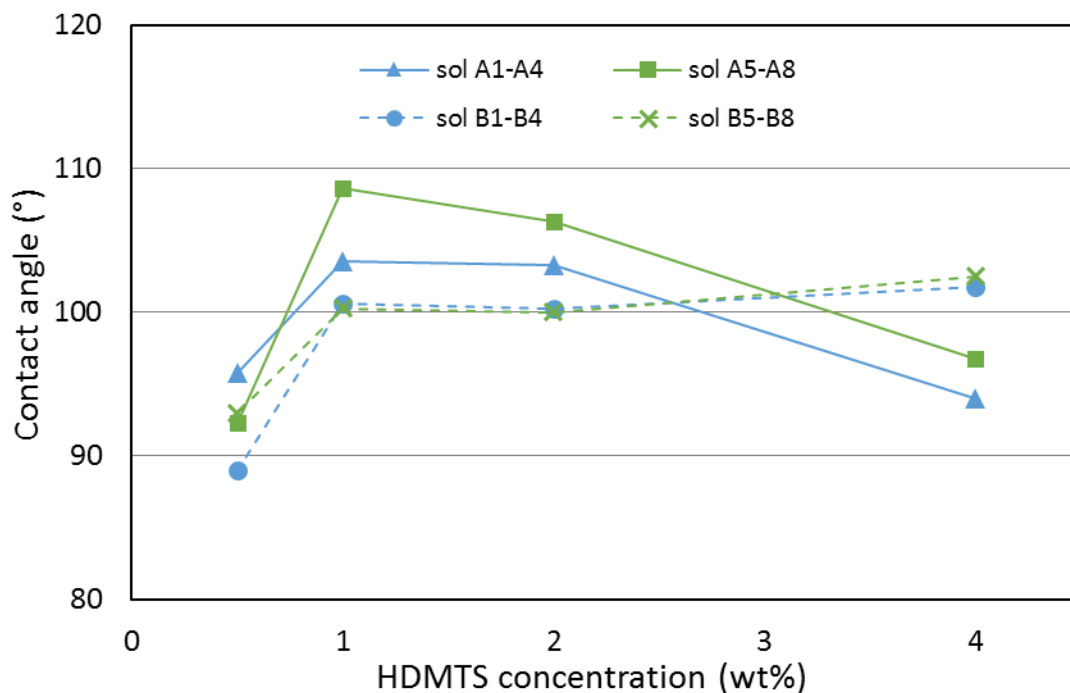
178

179 Considering the coating compositions with 4% HDTMS loading listed in Table 1, it was observed
180 that ethanol diluted sols (sol B series) performed better in terms of providing hydrophobicity to
181 hemp shiv surface compared to undiluted sols (sol A series). Sol B-1 and sol B-5 coatings had
182 higher contact angles (up to 105°) compared to sol A-1 and sol A-5 coatings (up to 100°).

183

184 Ethanol helps the HDTMS to be fully dissolved in water thereby promoting the hydrolysis
185 reaction [20,21]. Figure 2 shows the WCA measurements of sol coatings containing 4 wt%
186 HDTMS. Sol A-1 and sol A-5 contain only 4M ethanol whereas sol B-1 and sol B-5 contain
187 16M of ethanol. At 4 wt% HDTMS concentration, using 16M of ethanol favours the hydrolysis
188 of HDTMS. In this way HDTMS molecules are able to self-assemble on the silica network,
189 hence providing enhanced hydrophobicity to the material. In general, it was observed that sol-
190 gel coatings with HNO₃ as catalyst perform slightly better in terms of hydrophobicity than coatings
191 with HCl as catalyst.

192
193 The changes in water contact angle as a function of HDTMS loading (0.5-4.0 wt%) is presented
194 in Figure 3. The contact angle measurements had a standard deviation between 1.1° and 6.0°.
195 The hydrophobic performance of the coatings is not reduced on lowering the HDTMS loading
196 down to 1%. Surfaces coated with sol B series showed good water repellence with contact angles
197 ranging between 96° to 108°.



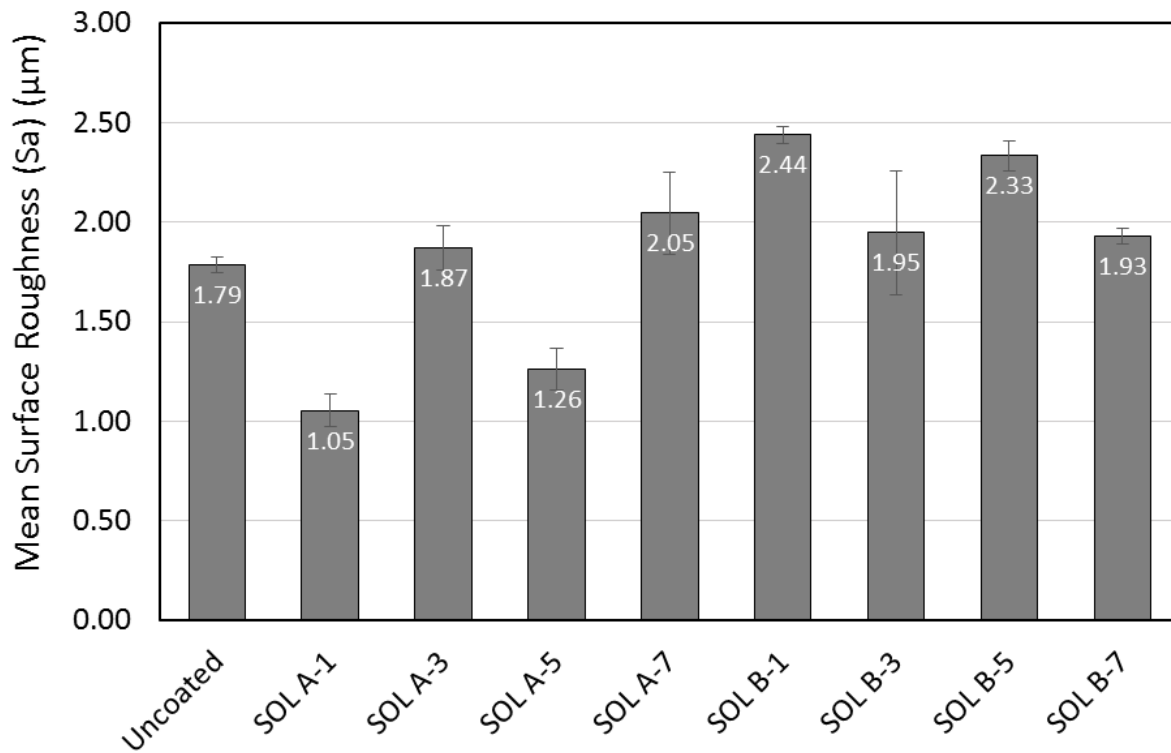
198
199 *Figure 3. Effect of ethanol dilution and varying HDTMS concentration in the sol-gel coating on hydrophobicity of hemp*
200 *shiv surface.*

201

202 3.2 Surface roughness of the coatings

203 The samples were analysed for their surface microstructure and roughness by the Vision64
204 software using a Robust Gaussian Filter (ISO 16610-31 2016) and a short wavelength cut-off
205 0.025mm. The use of such filters helps to reduce the anatomical influence and optimizes the
206 roughness profile data for evaluation of the sample surface [22,23]. The robust Gaussian filter
207 avoids the distortions produced by some filters when applied in profiles with deep valleys [24].
208 Mean surface roughness (S_a) was calculated according to ISO 4287 (1997). S_a gives the
209 description of the height variations in the surface and it is the most widely used parameter to
210 measure the surface roughness profile of the sample. The surface roughness parameters for sol-
211 gel coated hemp shiv with 1% and 4% HDTMS loadings are shown in Figure 4.

212



213

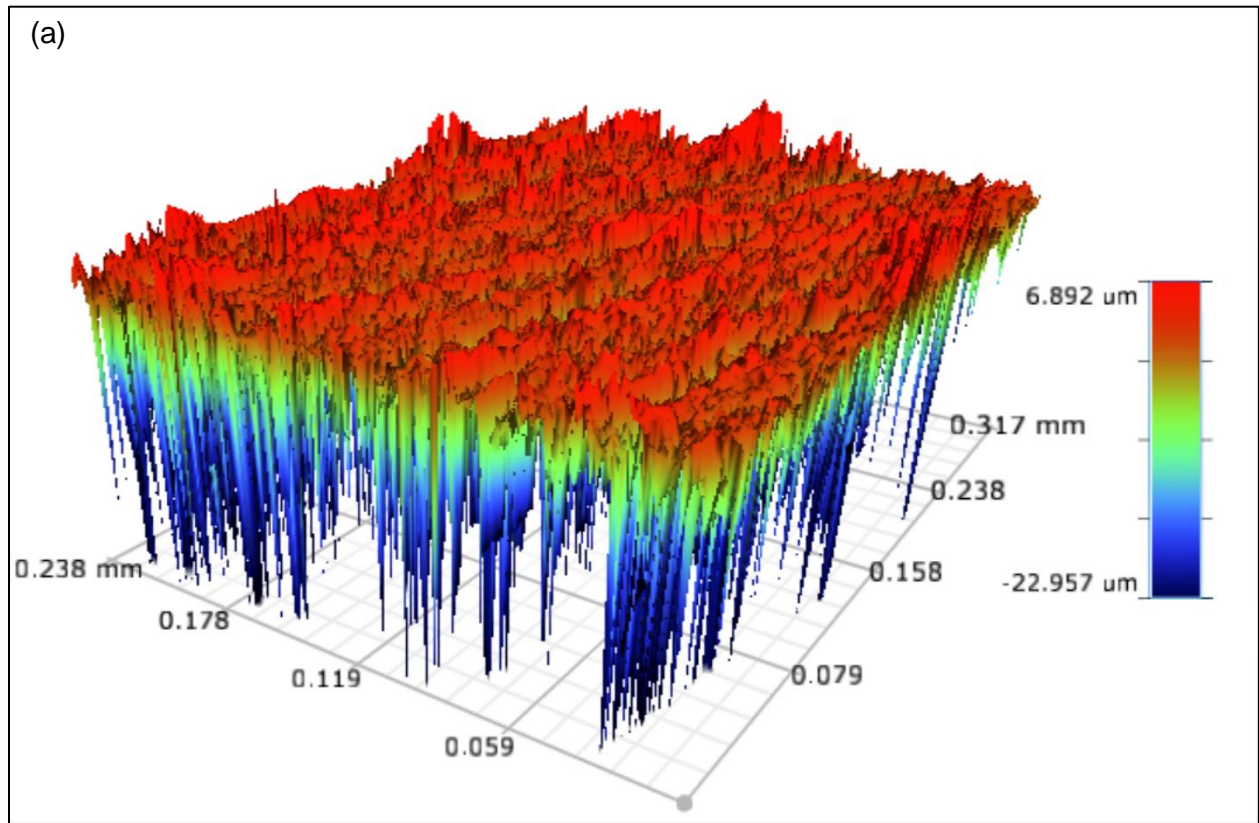
214 *Figure 4. Mean surface roughness (S_a) measurement of uncoated and sol-gel coated hemp shiv surfaces.*

215

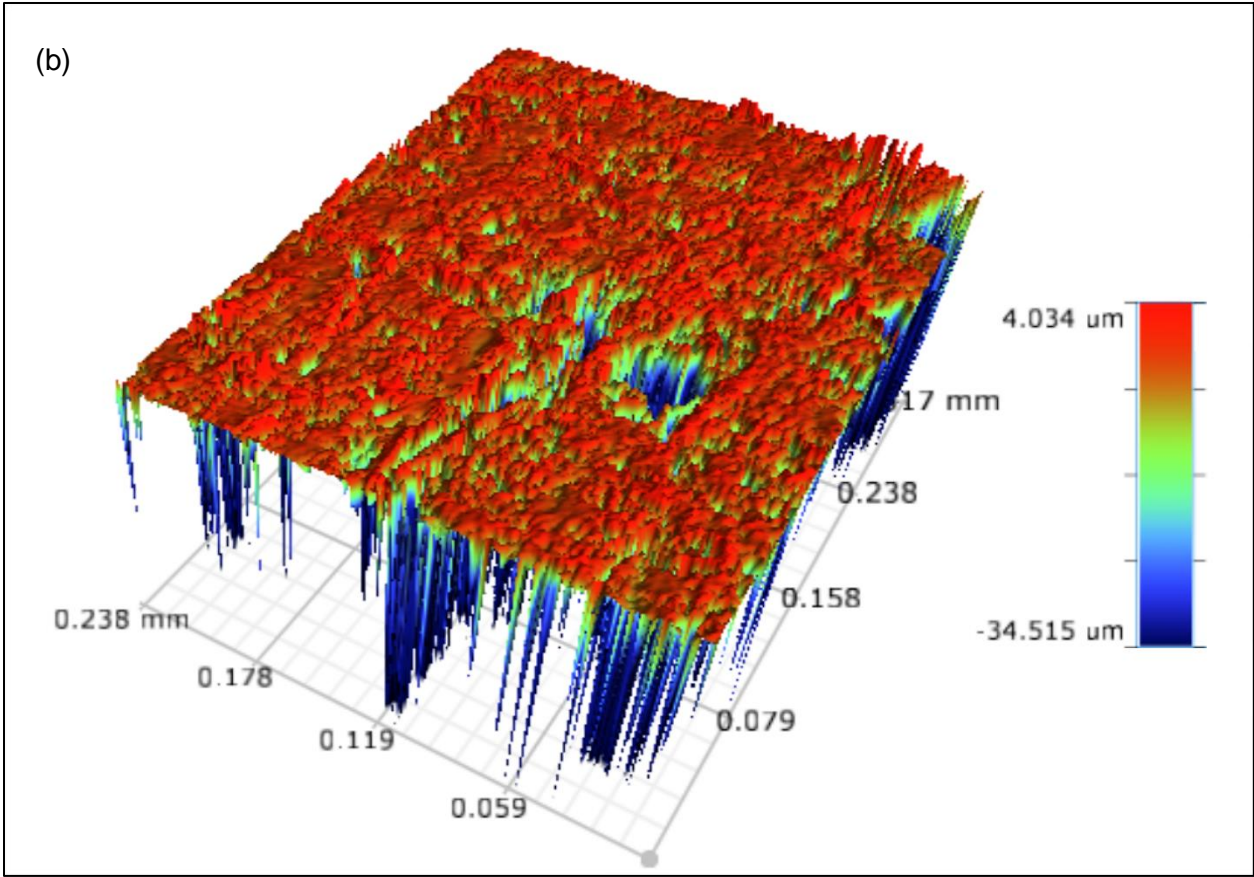
216 The influence of different sol-gel coatings on the surface roughness of hemp shiv can be seen in
217 Figure 5. The 3D surface roughness profile showed that the sol A-5 coating on the hemp shiv
218 lowered the surface roughness providing a smoother surface as seen in Figure 5b. The non-
219 uniform coating was also cracked, which in turn can facilitate water penetration into the hemp
220 shiv. On the other hand, sol A-7 (containing lower HDTMS loading) enhanced the surface

221 roughness of hemp shiv. Overall ethanol diluted sol-gel coatings had enhanced the surface
222 roughness of hemp shiv. Sol B-5 had the highest mean surface roughness as seen in Figure 5c.

223
224

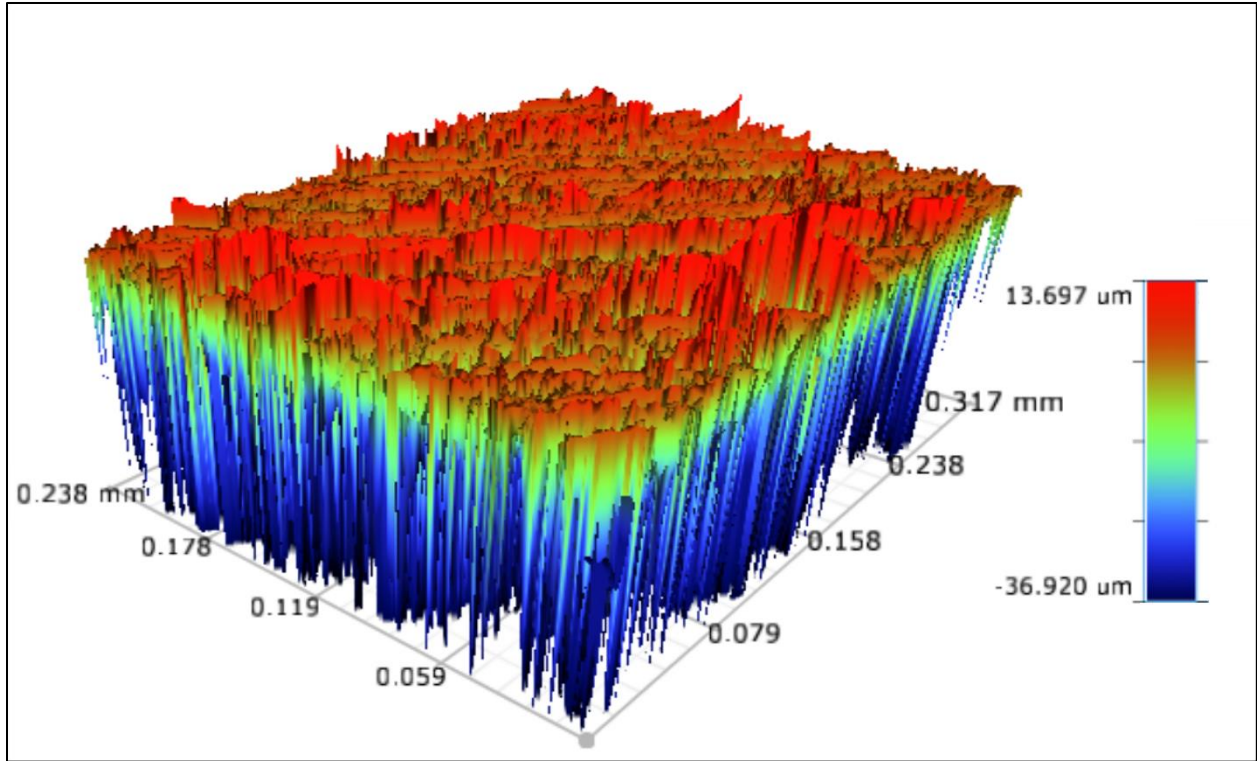


225



226
227
228

(c)



229

230

Figure 5. Surface roughness of (a) uncoated, (b) sol A-5 and (c) sol B-5 coated hemp shiv surface.

231

232 3.3 Surface Morphology

233

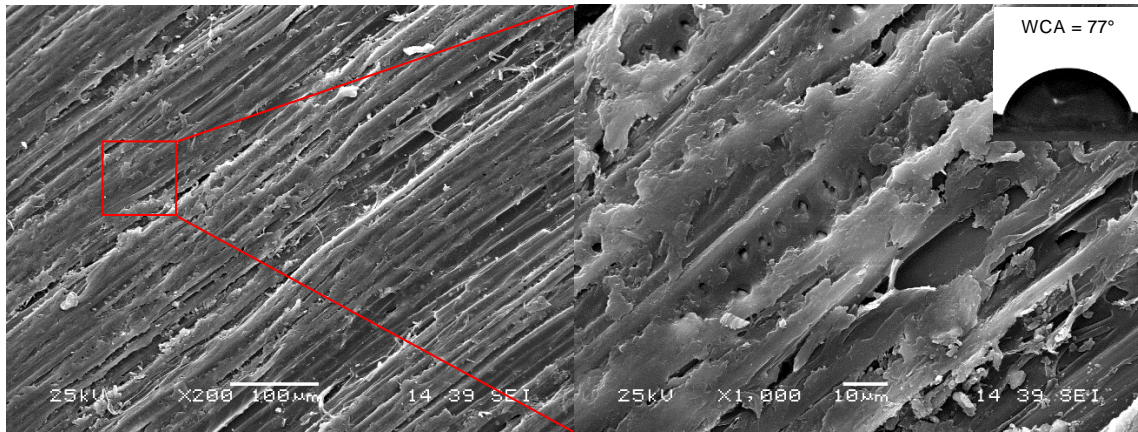
Roughness parameters alone cannot describe the surface morphology and therefore microscopy analysis is beneficial to improve surface evaluations. The morphology of the uncoated and sol-gel coated surfaces was studied by scanning electron microscopy (SEM). Figure 6 shows the micrographs of hemp shiv surface before and after modification with different sol-gel coatings. Sol A-5 and sol B-7 (Figures 6b and 6e) formed a thick coating layer and changed the morphology of the shiv surface. This resulted in coating with major cracks which could be a result of shrinkage after drying the treated sample (sol-gel coated hemp shiv). On the other hand, sol A-7 and sol B-5 (Figures 6c and 6d) showed uniformly coated surfaces without significantly altering the morphology of the hemp shiv.

242

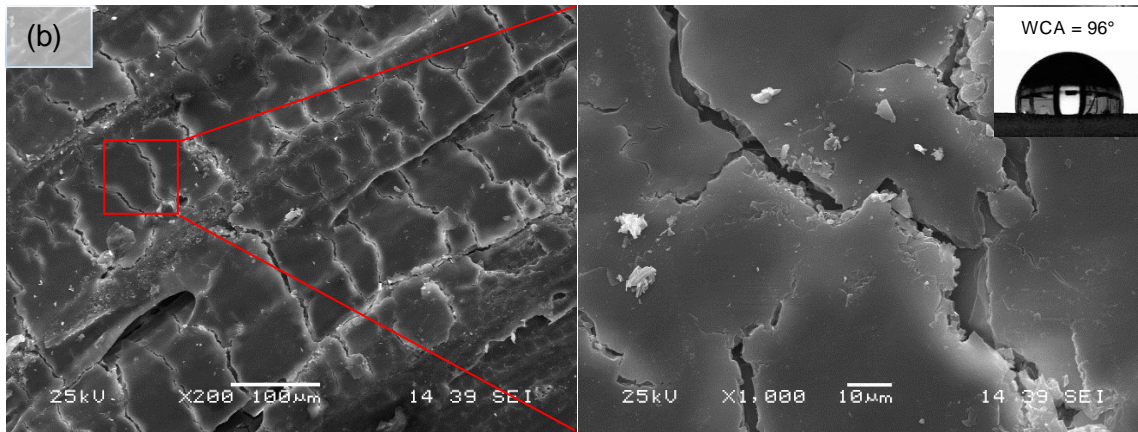
243

(a)

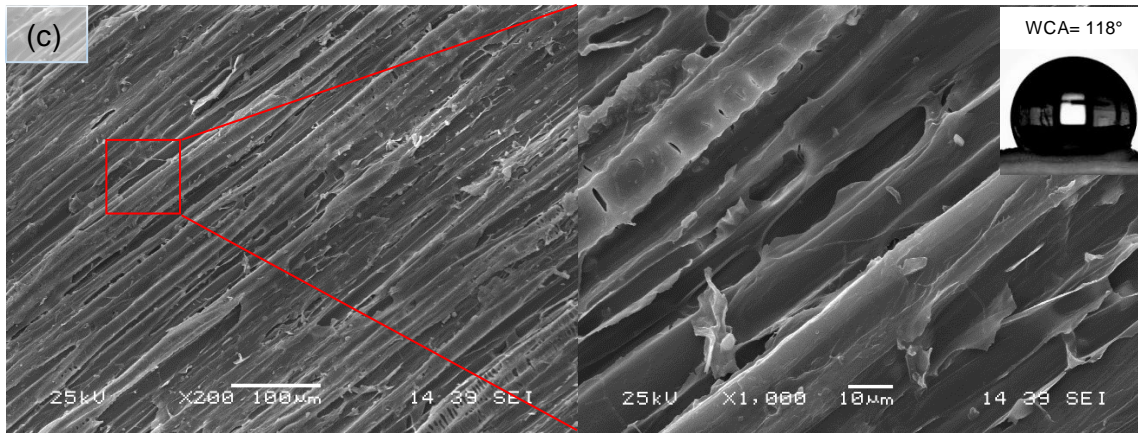
244
245



246
247

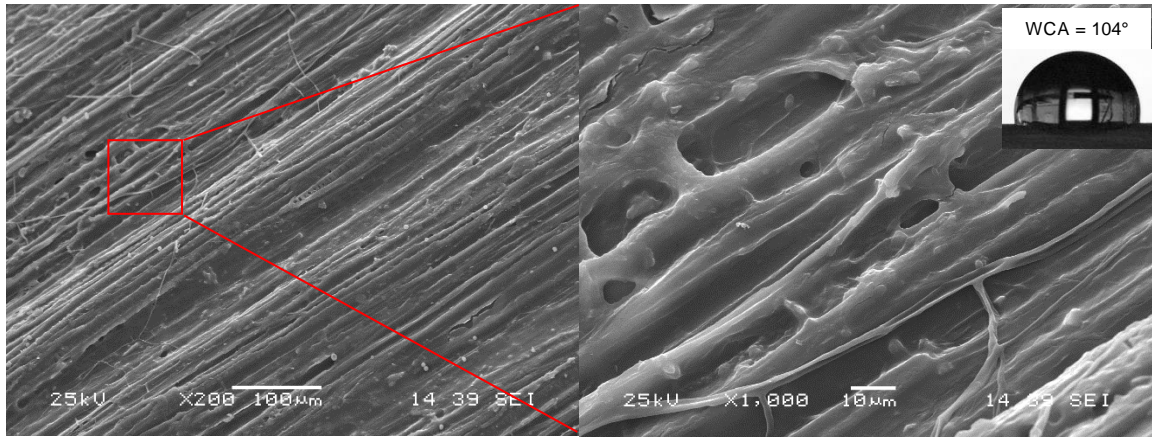


248
249

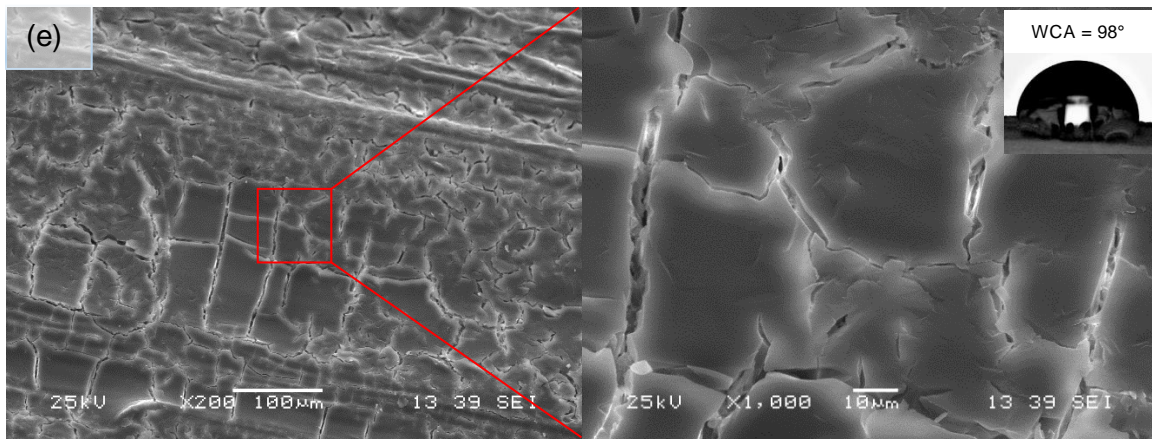


(d)

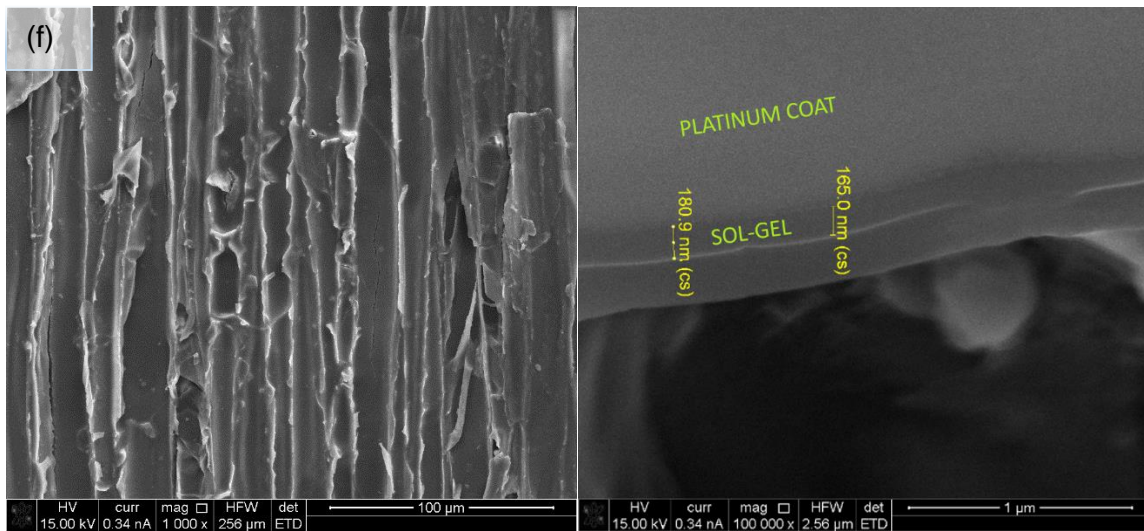
250
251



252
253



254



255 *Figure 6. Surface morphology and WCA of (a) uncoated, (b) sol A-5, (c) sol A-7, (d) sol B-5 (e) sol B-7 coated hemp*
256 *shiv surface and (f) thickness of sol-gel coating.*

257

258 Conventional SEM techniques proved unsuccessful in determining the coating thickness, but SEM-FIB
259 (Focused Ion Beam) imaging of an early iteration of the formulation (Figure 6f) measured a thickness in
260 the range 160-180nm. It is expected that the current formulations (sol A-7 and sol B-5) would have a
261 similar thickness.

262

263 **3.4 Chemical Composition**

264 The surface chemical composition was determined by X-ray photoelectron spectroscopy. A low-
265 resolution survey scan determined the atomic percentage of various elements present at the
266 sample surface (Figure 7). The relative elemental composition of the uncoated and sol-gel coated
267 hemp shiv surface is listed in Table 2.

268

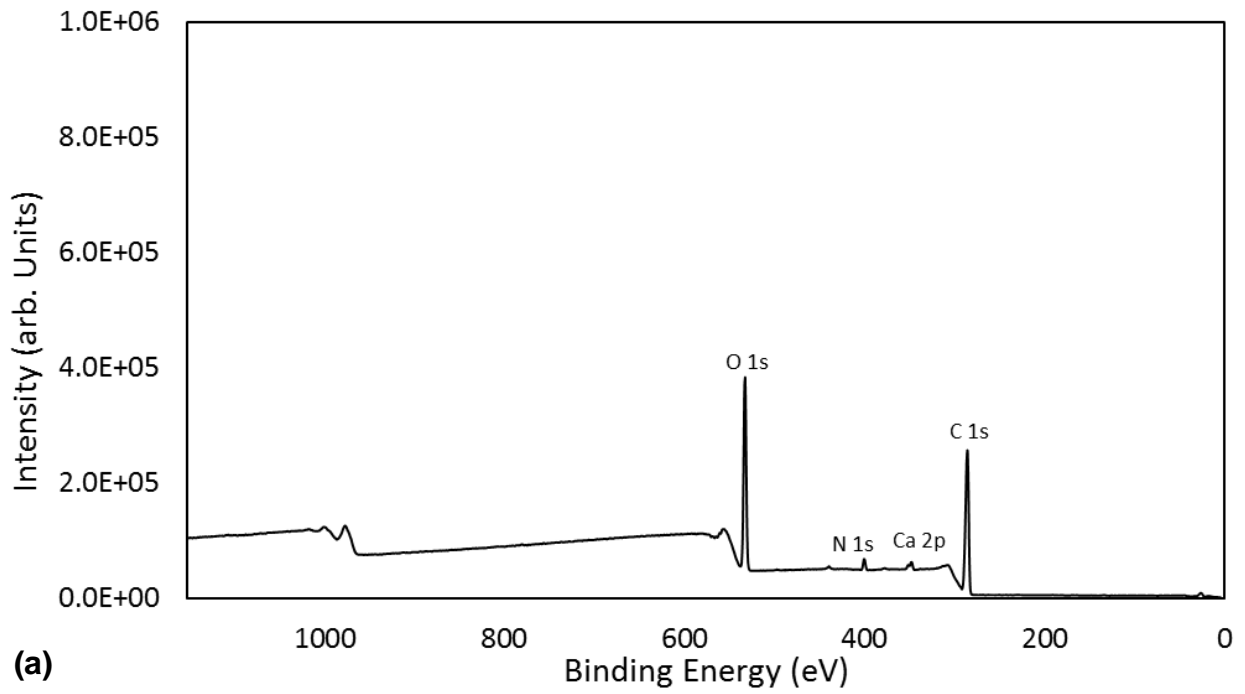
269 *Table 2. Relative amount of atoms at sample surface determined by low-resolution XPS scan.*

Element	Relative Conc. (atomic %)	
	Uncoated Hemp shiv	Sol A-7 Coated Hemp Shiv
C	69.61	28.33
O	27.06	53.57
N	2.06	-
Ca	0.64	-
P	0.14	-
K	0.30	-
S	0.09	-
Na	0.04	-
Cl	0.04	-
Co	0.03	-
Si	-	18.10

270

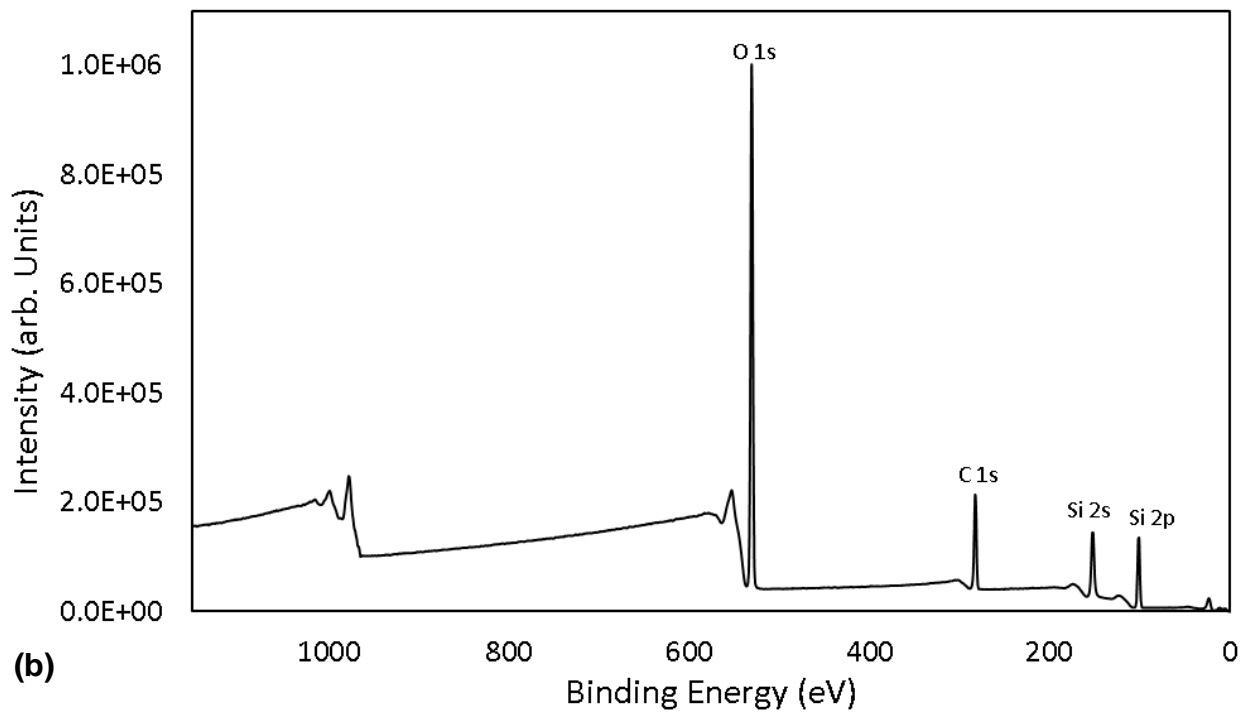
271 The main elements detected for uncoated hemp shiv were carbon and oxygen. Small amounts of
272 other elements were present either possibly arising from the epidermal cell wall or from
273 contamination during sample preparation. The sol-gel coated hemp shiv additionally showed high
274 content of silicon arising from the silica based membrane on the surface (Figure 7b).

275



276

277



278

279

Figure 7. XPS survey scan for (a) uncoated hemp shiv, (b) sol A-7 coated hemp shiv.

280

281 A high-resolution scan was performed on the C1s region for the uncoated and sol-gel coated
 282 hemp shiv samples to determine the type of oxygen-carbon bonds present. The chemical bond
 283 analysis of carbon was performed by curve-fitting the C1s peak and deconvoluting it into four sub
 284 peaks corresponding to unoxidized carbon C1, and various oxidized carbons C2, C3 and C4. A
 285 ratio between oxidized carbon (C_{ox}) and unoxidized carbon (C_{unox}) was calculated by the equation
 286 [25]:

$$288 \quad C_{ox/unox} = \frac{C_{ox}}{C_{unox}} = \frac{C2+C3+C4}{C1} \quad \text{Equation 1}$$

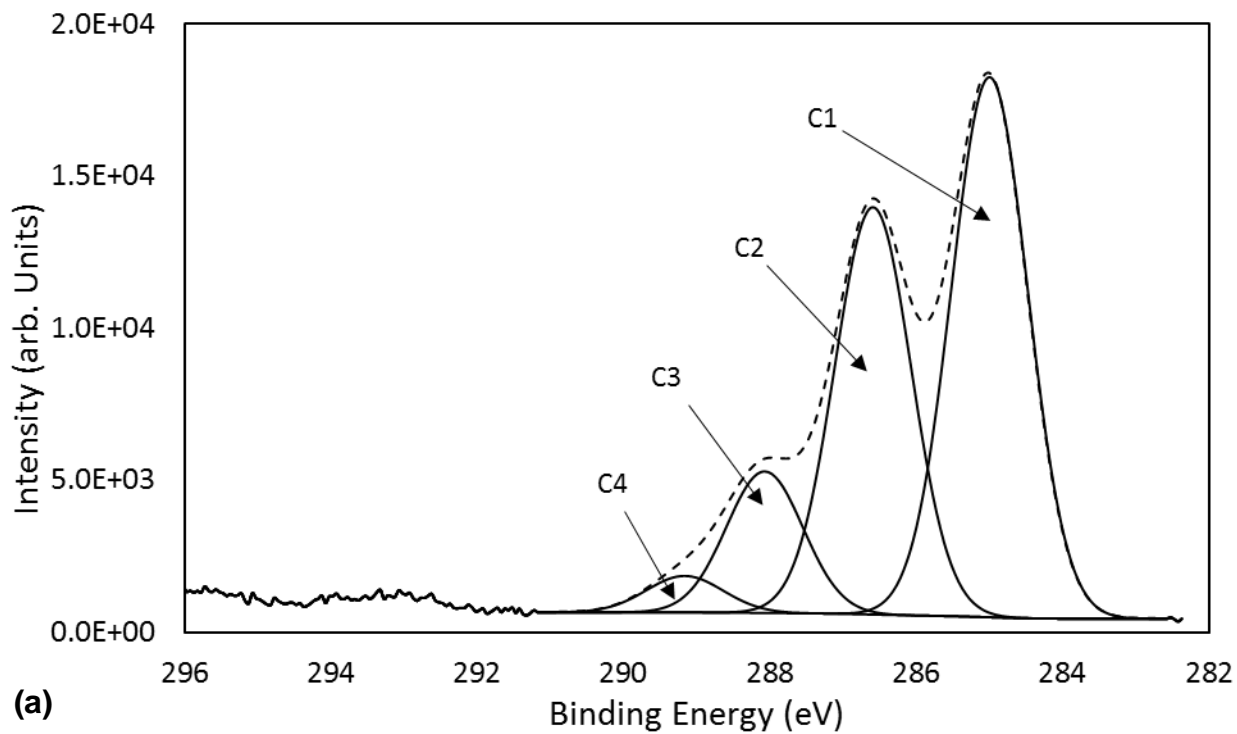
289
 290 The binding energy, corresponding bond type and their relative percentage are listed in Table 3.
 291 The ratio of $C_{ox/unox}$ has dropped significantly for sol-gel coated hemp shiv indicating that the
 292 carbon oxygen bonds have decreased on the surface of the samples.

293
 294 *Table 3. Deconvoluted peak parameters and relative amount of different carbon-to-oxygen bonds at sample surface*
 295 *determined by high-resolution XPS.*

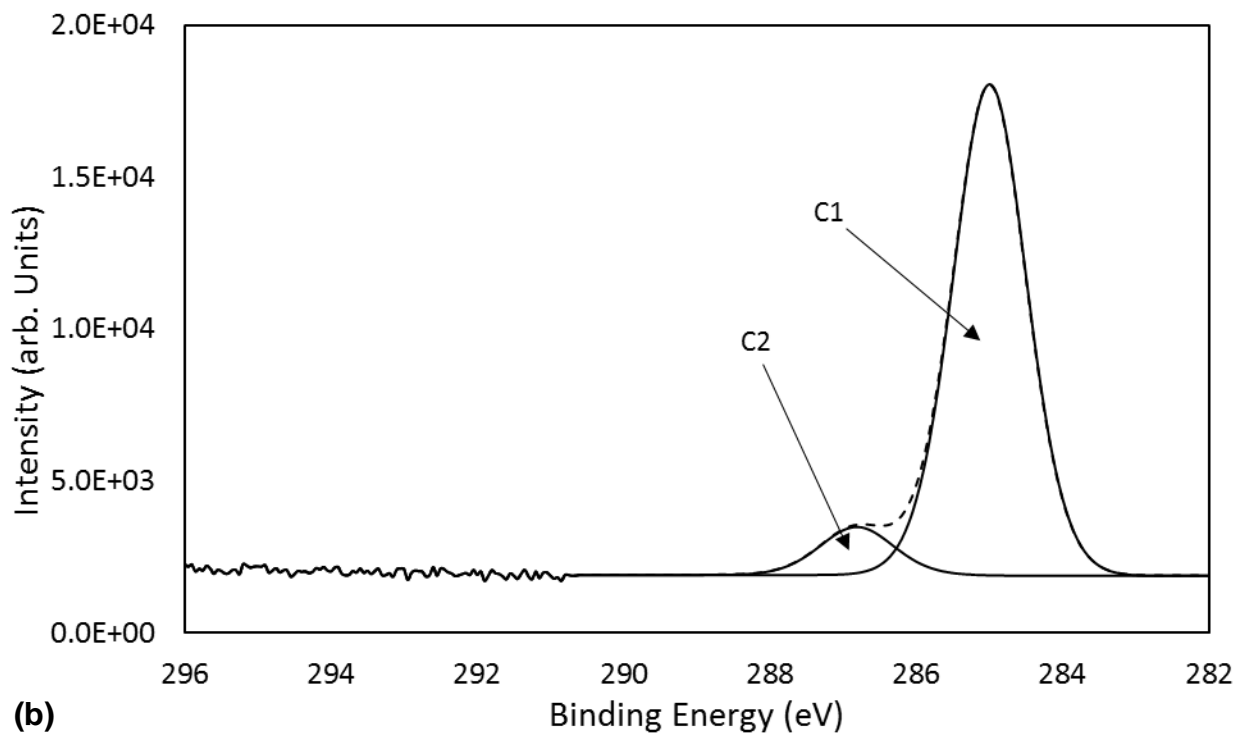
Carbon Group	Peak parameters		Relative amount (% area)	
	Binding Energy (eV)	Bond	Uncoated	Sol A-7 Coated
C1	285.0	C-C or C-H	48.01	91.09
C2	286.6/286.8	C-OH	36.18	8.91
C3	288.0	O-C-O or C=O	12.56	0.00
C4	289.2	O-C=O	3.24	0.00
$C_{ox/unox}$	-	-	1.08	0.09

296
 297 The C1s high resolution spectra with the deconvoluted peaks for uncoated and sol-gel coated
 298 surfaces are represented in Figure 8. The C1 peak represents carbon-carbon or carbon-hydrogen
 299 bonds whereas C2, C3, and C4 peaks possess carbon-oxygen bonds.

300
 301
 302



303
304

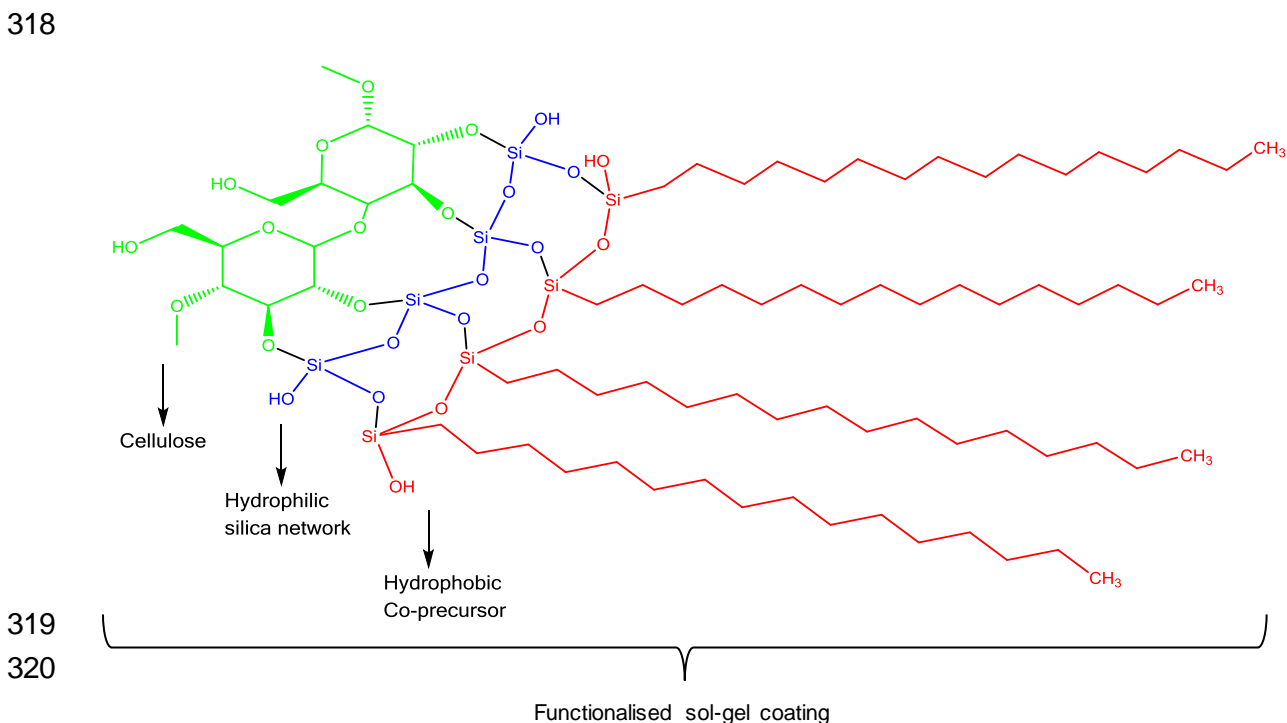


305
306
307

Figure 8. XPS scan of C_{1s} region for (a) uncoated hemp shiv, (b) sol A-7 coated hemp shiv.

308 **4. Discussion**

309 The sol-gel coatings were functionalised using HDTMS as the hydrophobic additive during the
310 sol-gel synthesis. The co-precursor method of sol-gel synthesis was followed based on the
311 simplicity of the process. In the sol-gel process, TEOS is hydrolysed and condensed to form a
312 SiO₂ network which is covalently bonded to cell wall through the hydroxyl sites of cellulose present
313 in the hemp shiv. On addition of hydrophobic agent as a co-precursor during the sol-gel
314 processing, the hydroxyl groups on the silica clusters are replaced by the –Si–C₁₆ groups through
315 oxygen bonds as illustrated in Figure 9. The hydrophobicity of the sol-gel coatings is due to the
316 attachment of these long alkyl chains on the silica network thereby providing water resistance to
317 the hemp shiv surface.



321 *Figure 9 Schematic illustration of sol-gel deposition on glucose units of cellulose.*

322

323 Overall, the acid catalysed sol-gel coatings enhance the water repellence of hemp shiv making
324 the surface hydrophobic (WCA>90°). The wettability of the surface is controlled by the surface
325 chemical composition as well as by the morphology of the microstructure. Surfaces with a similar
326 chemical composition may have different wettability behaviour due to the surface topology [26].
327 In this study, the surface of hemp shiv underwent microstructural changes via deposition of an
328 organo-functionalised silica coating.

329

330 Ethanol diluted sol series enhanced the surface roughness of the hemp shiv. At higher HDTMS
331 loading, undiluted coatings (sol A-1 and sol A-5) lowered the surface roughness of the shiv which
332 could explain the reason for lower contact angles compared to diluted coatings. Sol A-1 and sol
333 A-5 have HDTMS molecules that are not fully hydrolysed and being deposited onto the membrane
334 as a flat thick film as seen in Figure 6b. The reduced surface roughness can be attributed to the
335 extra HDTMS molecules on the coated surface [27].

336

337 Since an organic-inorganic hybrid coating was used, the ratio of TEOS: HDTMS was critical to
338 control the roughness of the coatings resulting in variable water repellent properties of the coated
339 hemp shiv. Most of the coatings enhanced the surface roughness except sol A-1 and sol A-5.
340 These coatings had smooth surfaces with cracks which could explain the lower contact angles
341 even though it had the highest loading of hydrophobic agent. It was observed that the TEOS:
342 HDTMS molar ratio in the coating formulations affected the hydrophobicity of the coated hemp
343 shiv. From Figure 3 it can be seen that varying the concentration of HDTMS in the formulations
344 affects the water contact angle. When TEOS: HDTMS was 1: 0.01 corresponding to 0.5 wt%
345 HDTMS, the contact angle was below 100° which suggests the concentration of the hydrophobic
346 agent was too low to provide sufficient level of hydrophobicity . The best results were obtained
347 with TEOS: HDTMS ratio 1: 0.02 (1 wt% HDTMS) with contact angles up to 118°. However, when
348 the TEOS: HDTMS ratio was increased to 1: 0.06 (4 wt% HDTMS), the hydrophobicity was
349 decreased for the undiluted sol coatings. These results can be explained by the combined effect
350 of surface roughness and energy. TEOS is hydrophilic whereas HDTMS is hydrophobic and
351 changing their molar ratio can affect the surface roughness and energy of the coated material.
352 Increasing the HDTMS concentration would reduce the surface energy. However the surface
353 roughness can be reduced if the HDTMS concentration is high enough as the extra silane fills the
354 inter-particle gap. Similar results have been reported in different coating systems [27,28].
355 Although sol B-7 coating enhanced the surface roughness, it had developed cracks which lowered
356 the water contact angle to 98°. The presence of surface cracks arising as a result of shrinkage
357 after drying the coated shiv is a significant factor to be considered when hydrophobic properties
358 are concerned. The hydrophobicity of modified hemp shiv can be compromised as the water
359 molecules can penetrate through the cracked coating wetting the bulk of the material over time.
360 Therefore, sol-gel coatings chemically modified the surface of hemp shiv which overall improved
361 the hydrophobicity of the material. The high water repellence can be attributed to the long alkyl
362 chains of HDTMS that provide high hydrophobicity.

363

364 The chemical composition of hemp shiv is mainly composed of cellulose, hemicellulose and lignin,
365 which altogether contain a large percentage of oxidized carbon in their structure. Hydroxyl groups
366 are known to contribute towards majority of the carbon-oxygen bonds in bio-based materials [29].
367 The XPS data confirmed that the sol-gel deposition on hemp shiv significantly altered the surface
368 chemistry. The surface carbon content of the coated hemp shiv decreased by 41.28% (from 69.61
369 to 28.33%). On the other hand, the oxygen content increased by 26.51% (from 27.06 to 53.57%).
370 This change in C/O ratio and increase in surface oxygen concentration can be attributed to O-
371 CH₃ bonds present in the polysiloxane coating on the surface of the sol-gel coated hemp shiv.
372 Moreover, the decrease in the surface carbon concentration of the sol-gel coated shiv can be
373 attributed to the masking effect of the polysiloxane coating which reduces the detectability of
374 surface cellulose and hemicellulose.

375

376 The C1s high resolution XPS spectra indicate that the surface has been modified by the silica
377 based coating that led to disappearance of C3 and C4 components of the C1s peaks. A shift in
378 the binding energy of C2 component (from 286.6 to 286.8 eV) was observed along with the
379 decrease in the intensity of the C2 component for the sol-gel coated sample. This shift indicates
380 the presence of a carbon atom linked to an oxygen and silicon atom (O-C-Si or C-O-Si) [18]. It
381 has also been shown [16,30–32] that curing above room temperature drives the dehydration
382 reaction at the adsorption sites between hydroxyl groups of the cellulose and the silanols forming
383 –Si-O-C- bonds. These bonds are formed by the linkage between polysilanol network with the
384 cellulose hydroxyl groups via polycondensation as illustrated in Figure 9. The increase in the
385 intensity of C1 component for sol-gel coated sample from 48.01% to 91.09% indicates the
386 presence of C-H and C-C bonds from the HDTMS hydrocarbon chain.

387

388 **5. Conclusion**

389 A simple one step dip-coating process was successfully applied to form a hydrophobic surface
390 onto an extremely hydrophilic bio-based aggregate construction material. The hydrophobic
391 properties were achieved through a combination of topological alteration and chemical
392 modification of the hemp shiv by the modified silica based sol-gel coatings.

393

394 The treated material (hemp shiv coated with silica based membrane) delivered the following
395 properties when compared to the untreated hemp shiv:

- 396 • Delivered water repellence by maintaining stable water contact angles over 60 seconds.
- 397 • Controlled surface wettability through microstructure modification.
- 398 • Uniform and crack-free coated surface.
- 399 • Enhanced surface roughness providing water contact angles up to 118°.

400

401 It can be concluded that water based sol-gel coatings with low HDTMS precursor loading (sol A-
402 7) would be of interest to the bio-based building industry due to its hygroscopic properties, long
403 shelf life, reduced cost and lower environmental impact.

404

405 **Acknowledgments**

406 This study was supported by the Canadian Queen Elizabeth II Diamond Jubilee Scholarship and
407 the ISOBIO project funded by the Horizon 2020 programme [grant number 636835 – ISOBIO –
408 H2020-EeB-2014-2015]. The authors would also like to acknowledge the EPSRC Centre for
409 Decarbonisation of the Built Environment (dCarb) [grant number EP/L016869/1] and the NSERC
410 project (grant number IRCPJ 461745-12). The ISOBIO project aims to develop and bring new bio-
411 based insulation panels and renders into the mainstream for the purpose of creating more energy
412 efficient buildings. The contents of this publication are the sole responsibility of the authors and
413 can in no way be taken to reflect the views of the European Union.

414

415 **References**

- 416 [1] J. Genzer, K. Efimenko, Recent developments in superhydrophobic surfaces and their
417 relevance to marine fouling: a review., *Biofouling*. 22 (2006) 339–360.
418 doi:10.1080/08927010600980223.
- 419 [2] A. Nakajima, K. Hashimoto, T. Watanabe, Recent studies on super-hydrophobic films, in:
420 *Monatshefte Fur Chemie*, 2001: pp. 31–41. doi:10.1007/s007060170142.
- 421 [3] S. Benfratello, C. Capitano, G. Peri, G. Rizzo, G. Scaccianoce, G. Sorrentino, Thermal and
422 structural properties of a hemp-lime biocomposite, *Constr. Build. Mater.* 48 (2013) 745–
423 754. doi:10.1016/j.conbuildmat.2013.07.096.
- 424 [4] A.D. Tran Le, C. Maalouf, T.H. Mai, E. Wurtz, F. Collet, Transient hygrothermal behaviour
425 of a hemp concrete building envelope, *Energy Build.* 42 (2010) 1797–1806.
426 doi:10.1016/j.enbuild.2010.05.016.
- 427 [5] L. Arnaud, E. Gourlay, Experimental study of parameters influencing mechanical properties

- 428 of hemp concretes, *Constr. Build. Mater.* 28 (2012) 50–56.
429 doi:10.1016/j.conbuildmat.2011.07.052.
- 430 [6] M. Theis, B. Grohe, Biodegradable lightweight construction boards based on
431 tannin/hexamine bonded hemp shaves, *Holz Als Roh - Und Werkst.* 60 (2002) 291–296.
432 doi:10.1007/s00107-002-0306-0.
- 433 [7] H. Kyma, M. Hautala, R. Kuisma, A. Pasila, Capillarity of flax / linseed (*Linum usitatissimum*
434 L.) and fibre hemp (*Cannabis sativa* L.) straw fractions, 14 (2001) 41–50.
- 435 [8] J. Gassan, V.S. Gutowski, A.K. Bledzki, About the surface characteristics of natural fibres,
436 *Surf. Eng.* 283 (2000) 132–139. doi:10.1002/1439-2054(20001101)283:1<132::AID-
437 MAME132>3.0.CO;2-B.
- 438 [9] S. Marceau, P. Glé, M. Guéguen-Minerbe, E. Gourlay, S. Moscardelli, I. Nour, S. Amziane,
439 Influence of accelerated aging on the properties of hemp concretes, *Constr. Build. Mater.*
440 139 (2017) 524–530. doi:10.1016/j.conbuildmat.2016.11.129.
- 441 [10] L. Kidalova, N. Stevulova, E. Terpakova, Influence of water absorption on the selected
442 properties of hemp hurds composites, *Pollack Period.* (2015).
443 doi:10.1556/Pollack.10.2015.1.12.
- 444 [11] M.R. Vignon, D. Dupeyre, Steam explosion of woody hemp ch nevotte, 17 (1995) 395–
445 404.
- 446 [12] M.M. Kabir, H. Wang, K.T. Lau, F. Cardona, Chemical treatments on plant-based natural
447 fibre reinforced polymer composites: An overview, *Compos. Part B Eng.* 43 (2012) 2883–
448 2892. doi:10.1016/j.compositesb.2012.04.053.
- 449 [13] S. Donath, H. Militz, C. Mai, Wood modification with alkoxysilanes, *Wood Sci. Technol.* 38
450 (2004) 555–566. doi:10.1007/s00226-004-0257-1.
- 451 [14] E. Cabane, T. Keplinger, V. Merk, P. Hass, I. Burgert, Renewable and functional wood
452 materials by grafting polymerization within cell walls, *ChemSusChem.* 7 (2014) 1020–1025.
453 doi:10.1002/cssc.201301107.
- 454 [15] J. Song, O.J. Rojas, Approaching super-hydrophobicity from cellulosic materials: A
455 Review, *Pap. Chem.* 28 (2013) 216–238. doi:10.3183/NPPRJ-2013-28-02-p216-238.
- 456 [16] A. Valadez-Gonzalez, J.M. Cervantes-Uc, R. Olayo, P.J. Herrera-Franco, Effect of fiber
457 surface treatment on the fiber-matrix bond strength of natural fiber reinforced composites,
458 *Compos. Part B Eng.* 30 (1999) 309–320. doi:10.1016/S1359-8368(98)00054-7.
- 459 [17] C. Brinker, G. Scherer, *Sol-Gel Science: The Physics and Chemistry of Sol-Gel*
460 *Processing*, *Adv. Mater.* 3 (1990) 912. doi:10.1186/1471-2105-8-444.
- 461 [18] M.A. Tshabalala, P. Kingshott, M.R. Vanlandingham, D. Plackett, Surface Chemistry and

- 462 Moisture Sorption Properties of Wood Coated with Multifunctional Alkoxysilanes by Sol-
463 Gel Process, (2002).
- 464 [19] B. Tomšič, B. Simončič, B. Orel, L. Černe, P.F. Tavčer, M. Zorko, I. Jerman, A. Vilčnik, J.
465 Kovač, Sol-gel coating of cellulose fibres with antimicrobial and repellent properties, *J.*
466 *Sol-Gel Sci. Technol.* 47 (2008) 44–57. doi:10.1007/s10971-008-1732-1.
- 467 [20] L. Xu, W. Zhuang, B. Xu, Z. Cai, Superhydrophobic cotton fabrics prepared by one-step
468 water-based sol-gel coating, *J. Text. Inst.* 103 (2012) 311–319.
469 doi:10.1080/00405000.2011.569238.
- 470 [21] S. Sankaraiah, J.M. Lee, J.H. Kim, S.W. Choi, Preparation and characterization of surface-
471 functionalized polysilsesquioxane hard spheres in aqueous medium, *Macromolecules.* 41
472 (2008) 6195–6204. doi:10.1021/ma8003345.
- 473 [22] Y. Fujiwara, Y. Fujii, Y. Sawada, S. Okumura, Assessment of wood surface roughness:
474 Comparison of tactile roughness and three-dimensional parameters derived using a robust
475 Gaussian regression filter, *J. Wood Sci.* 50 (2004) 35–40. doi:10.1007/s10086-003-0529-
476 7.
- 477 [23] L. Gurau, H. Mansfield-Williams, M. Irle, Filtering the roughness of a sanded wood surface,
478 *Holz Als Roh - Und Werkst.* 64 (2006) 363–371. doi:10.1007/s00107-005-0089-1.
- 479 [24] B. Ugulino, R.E. Hernández, Assessment of surface properties and solvent-borne coating
480 performance of red oak wood produced by peripheral planing, *Eur. J. Wood Wood Prod.*
481 (2016) 1–13. doi:10.1007/s00107-016-1090-6.
- 482 [25] N.M. Stark, L.M. Matuana, Surface chemistry changes of weathered HDPE/wood-flour
483 composites studied by XPS and FTIR spectroscopy, *Polym. Degrad. Stab.* 86 (2004) 1–9.
484 doi:10.1016/j.polymdegradstab.2003.11.002.
- 485 [26] Q.F. Xu, J.N. Wang, K.D. Sanderson, Organic-inorganic composite nanocoatings with
486 superhydrophobicity, good transparency, and thermal stability, *ACS Nano.* 4 (2010) 2201–
487 2209. doi:10.1021/nn901581j.
- 488 [27] H. Wang, H. Zhou, S. Liu, H. Shao, S. Fu, G.C. Rutledge, T. Lin, Durable, self-healing,
489 superhydrophobic fabrics from fluorine-free, waterborne, polydopamine/alkyl silane
490 coatings, *RSC Adv.* 7 (2017) 33986–33993. doi:10.1039/C7RA04863G.
- 491 [28] C. Zeng, H. Wang, H. Zhou, T. Lin, Self-cleaning, superhydrophobic cotton fabrics with
492 excellent washing durability, solvent resistance and chemical stability prepared from an
493 SU-8 derived surface coating, *RSC Adv.* 5 (2015) 61044–61050.
494 doi:10.1039/C5RA08040A.
- 495 [29] N.M. Stark, L.M. Matuana, Ultraviolet weathering of photostabilized wood-flour-filled high-

- 496 density polyethylene composites, *J. Appl. Polym. Sci.* 90 (2003) 2609–2617.
497 doi:10.1002/app.12886.
- 498 [30] Y. Xie, C.A.S. Hill, Z. Xiao, H. Miltz, C. Mai, Silane coupling agents used for natural
499 fiber/polymer composites: A review, *Compos. Part A Appl. Sci. Manuf.* 41 (2010) 806–819.
500 doi:10.1016/j.compositesa.2010.03.005.
- 501 [31] M. Castellano, A. Gandini, P. Fabbri, M.N. Belgacem, Modification of cellulose fibres with
502 organosilanes: Under what conditions does coupling occur?, *J. Colloid Interface Sci.* 273
503 (2004) 505–511. doi:10.1016/j.jcis.2003.09.044.
- 504 [32] M. Abdelmouleh, S. Boufi, M.N. Belgacem, A. Dufresne, Short natural-fibre reinforced
505 polyethylene and natural rubber composites: Effect of silane coupling agents and fibres
506 loading, *Compos. Sci. Technol.* 67 (2007) 1627–1639.
507 doi:10.1016/j.compscitech.2006.07.003.
508